Citation: Molecular Therapy–Nucleic Acids (2013) 2, e85; doi:10.1038/mtna.2013.15

www.nature.com/mtna

METHODS: ORIGINAL ARTICLE

RANGE: Gene Transfer of Reversibly Controlled Polycistronic Genes

Yiwei Chen[1], Liji Cao[2], Chonglin Luo[3], Désirée AW Ditzel[1], Jörg Peter[2] and Rolf Sprengel[1]

We developed a single vector recombinant adeno-associated viral (rAAV) expression system for spatial and reversible control of polycistronic gene expression. Our approach (i) integrates the advantages of the tetracycline (Tet)-controlled transcriptional silencer tTS^{Kid} and the self-cleaving 2A peptide bridge, (ii) combines essential regulatory components as an autoregulatory loop, (iii) simplifies the gene delivery scheme, and (iv) regulates multiple genes in a synchronized manner. Controlled by an upstream Tet-responsive element (TRE), both the ubiquitous chicken β-actin promoter (CAG) and the neuron-specific synapsin-1 promoter (Syn) could regulate expression of tTS^{Kid} together with two 2A-linked reporter genes. Transduction *in vitro* exhibited maximally 50-fold regulation by doxycycline (Dox). Determined by gene delivery method as well as promoter, highly specific tissues were transduced *in vivo*. Bioluminescence imaging (BLI) visualized reversible "ON/OFF" gene switches over repeated "Doxy-Cycling" in living mice. Thus, the reversible rAAV-mediated N-cistronic gene expression system, termed RANGE, may serve as a versatile tool to achieve reversible polycistronic gene regulation for the study of gene function as well as gene therapy.

Molecular Therapy–Nucleic Acids (2013) **2**, e85; doi:10.1038/mtna.2013.15; published online 9 April 2013
Subject Category: Methods

Introduction

Viral vectors are valuable tools for transfer and expression of heterologous genes *in vivo*.[1,2] Recent advances in recombinant adeno-associated viral (rAAV) vectors have facilitated the production of high purity, high titer, and helper virus-free vector stocks.[3,4] Such purified replication-deficient rAAV vectors efficiently deliver long-term gene expression to target tissues with reduced toxicity and immune response compared with most other viral vector systems.[1,2] Unlike retroviral vectors, rAAV infects both dividing and nondividing cells, and persists in an extrachromosomal (episomal) state without integrating into the host genome.[1,2] Although long-term rAAV-mediated gene expression is desired, the regulation of heterologous gene expression in target cells is critical for correlating phenotypes in gene function analysis, as well as for the adjustment of gene expression in gene therapy.

Among several regulated gene expression systems, the tetracycline (Tet)-controlled system holds promise for regulating rAAV gene expression. The Tet system was developed from prokaryotes, and has no known pleiotropic effects in eukaryotes.[5,6] In contrast to recombination-based systems, the Tet system controls gene expression at the transcriptional level in response to Tet, permitting adjustable and reversible gene regulation.[7] The Tet system has been adapted to all major model organisms, facilitating physiological studies at the cellular level and detailed analysis of complex biological processes such as development, behavior, and disease.[8]

The rAAV-mediated Tet-controlled gene system has been successfully applied to various tissue types, including liver,[9] brain,[10,11] and retina.[12–15] rAAVs have demonstrated robust Tet-responsive gene expression; however, significant levels of background expression in uninduced "OFF" states were frequently observed.[9,10] Because of its binary design, rAAV gene regulation by Tet was originally delivered by two rAAV vectors: one that expresses a Tet-controlled transactivator[16–18] or silencer[12,19] under a cellular promoter, and a second that expresses a gene of interest controlled by a synthetic Tet-responsive promoter. A limitation is that the two promoters can behave differently upon transduction, leading to unpredictable divergent expression patterns and differential expression kinetics.[11,20] To ensure simultaneous gene delivery, many efforts have been made to accommodate essential Tet regulatory components in a single vector configuration by using multiple[13–15] or bidirectional[9,10] Tet-responsive promoters. Most importantly, an ideal design has to provide a balance between the limited AAV packaging capacity (~5 kb) and efficient Tet-responsive regulation.

We describe here a novel single vector rAAV system (termed RANGE for **r**eversible r**A**AV-mediated **N**-cistronic **g**ene **e**xpression system) for spatial and reversible polycistronic gene expression. First, we validated *in vitro* the functionality and characterized the RANGE system in detail. We then delivered RANGE to living mice through focal or systemic rAAV administration, and demonstrated highly tissue-specific RANGE in mice. Reversibility of RANGE was visualized *in vivo* by noninvasive bioluminescence imaging (BLI). Our results suggest that RANGE may serve in future as a broadly applicable tool to obtain regulatable polycistronic expression for gene study as well as multitargeted gene therapy.

[1]Department of Molecular Neurobiology, Max Planck Institute for Medical Research, Heidelberg, Germany; [2]Division of Medical Physics in Radiology (E020), German Cancer Research Center (DKFZ), Heidelberg, Germany; [3]Division of Translational Immunology (D015), German Cancer Research Center (DKFZ), Heidelberg, Germany. Correspondence: Rolf Sprengel, Department of Molecular Neurobiology, Max Planck Institute for Medical Research, Jahnstrasse 29, D-69120 Heidelberg, Germany. E-mail: rolf.sprengel@mpimf-heidelberg.mpg.de
Keywords: 2A peptide bridge; conditional gene expression; rAAV; Tet system
Received 12 December 2012; accepted 11 February 2013; advance online publication 9 April 2013. doi:10.1038/mtna.2013.15

Results

Design of a conditional polycistronic gene expression system

In our experimental design, we took advantage of the Tet-controlled transcriptional silencer tTS^{Kid}, a fusion protein of a prokaryotic Tet repressor (tetR) domain and a Krüppel-associated box (KRAB) domain derived from rat kidney protein Kid-1.[21] The KRAB domain is present in about one-third of zinc finger proteins and has been found to be a potent transcriptional repressor domain.[22,23] To control eukaryotic gene expression machinery by tTS^{Kid}, the Tet-responsive element (TRE) is placed upstream of the RNA polymerase II promoter. TRE contains seven repeats of Tet operator sequences, which serve as the binding site for the tetR domain. Using T2A peptide bridges derived from *Thosea asigna* virus,[24] several genes are linked in frame and coexpressed with tTS^{Kid}.

The core system of RANGE works in two modes (**Figure 1a**): (i) in the absence of doxycycline (Dox), transcription of all genes including tTS^{Kid} is driven by a RNA polymerase II promoter. Once tTS^{Kid} has bound to TRE *via* tetR, the Kid domain represses the activity of the downstream promoter. Therefore, expression of all genes including tTS^{Kid} is repressed through an autoregulatory loop. (ii) In the presence of Dox, Dox binds to tTS^{Kid} and reduces its affinity to TRE, and thus attenuates tTS^{Kid}-TRE binding. The downstream promoter is thus relieved from Kid silencing, and initiates transcription of all genes as a single mRNA. During translation, 2A peptide bridges mediate self-cleavage through a "ribosomal skipping" mechanism, leading to polycistronic expression of all 2A-linked genes.[25]

In contrast to the classical Tet systems (tTA or rtTA) that are based on transactivation of a synthetic promoter,[16,18] the RANGE system regulates the cellular promoter between a repressed "OFF" state and an "ON" state in which promoter activity is regained. This occurs when Dox inactivates tTS^{Kid} repression, resulting in reduced basal activity in the "OFF" state. Once Dox is eliminated, RANGE is turned down by rebinding of tTS^{Kid} to TRE.

For qualitative and quantitative characterization of the RANGE system, we cloned the tTS^{Kid} gene between two reporter genes: firefly luciferase (Fluc) and fluorescent protein mKO (monomeric Kusabira-Orange).[26] Two promoters were analyzed: the ubiquitous cytomegalovirus (CMV) early enhancer/chicken β-actin promoter (CAG)[27] and the neuron-specific human synapsin-1 promoter (Syn).[28] The expression cassettes were anchored in an rAAV backbone.[29] As a control for each TRE promoter, an identical vector was generated without TRE sequences (constitutive vector; **Figure 1a**).

Conditional polycistronic gene expression *in vitro*

In transiently transfected HEK 293 cells, mKO fluorescence indicated expression of the polycistrons. In those cells transfected with the conditional TRE constructs, mKO levels were low without Dox and markedly higher upon Dox treatment. In contrast, mKO levels did not exhibit Dox-dependence in the cells transfected with the constitutive constructs lacking TRE (**Figure 1b**). The Dox-induced increase in Fluc levels were 1.7-fold (± 0.1) for the CAG and 3.8-fold (± 0.1) for the Syn promoter when controlled by TRE, whereas Dox without TRE failed to regulate Fluc (CAG: $P = 0.37$; Syn: $P = 0.90$) (**Figure 1c**). The polycistron-encoded cytoplasmic Fluc (63 kDa) and nuclear-targeted tTS^{Kid} (34 kDa) were simultaneously detected by western blot analysis using an anti-2A antibody (**Figure 1d**). Moreover, expression of tTS^{Kid} was also subjected to Dox regulation, and limited to lower Fluc levels when the system is in the "OFF" state. This confirms the autoregulatory feature of RANGE, and implies that low levels of tTS^{Kid} are sufficient to keep the system at the "OFF" state.

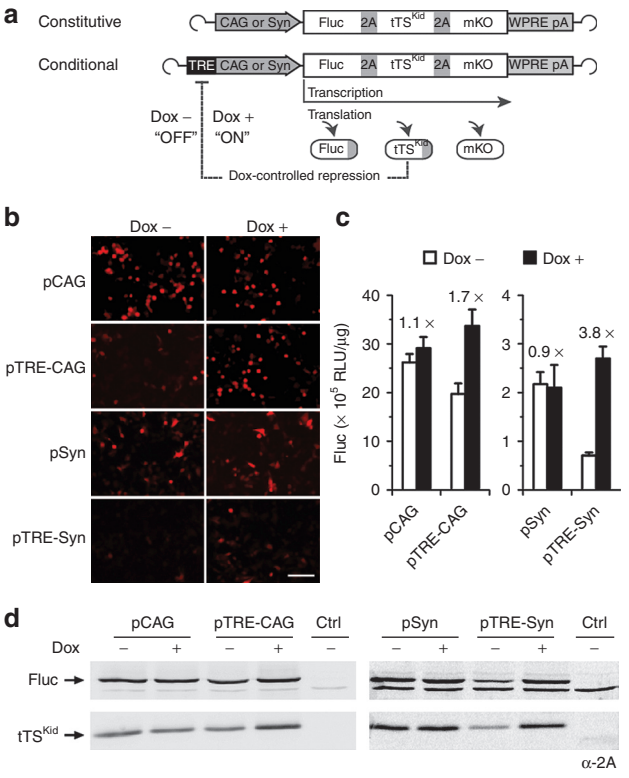

Figure 1 The RANGE system. (**a**) Schematic view of the Dox-controlled polycistronic gene expression system. A eukaryotic promoter, CAG or Syn, drives polycistronic expression of tTS^{Kid} together with two 2A-linked reporter genes, firefly luciferase (Fluc) and fluorescent protein mKO. Without Dox, the tetR domain of tTS^{Kid} binds to TRE, and tTS^{Kid} represses the activity of TRE-controlled promoter. Thus, expression of Fluc, mKO as well as tTS^{Kid} itself are repressed *via* an autoregulatory loop. In the presence of Dox, Dox binds to tTS^{Kid}, thus preventing tTS^{Kid}-TRE interaction. The TRE-controlled promoter is relieved from repression, and transcribes the genes as a single mRNA. The 2A sequences mediate self-cleavage during translation, leading to coexpression of Fluc, tTS^{Kid}, and mKO. (**b**) Fluorescence images of HEK 293 cells transfected with tTS^{Kid}-based constructs 48 hours after transfection in the absence or presence of Dox (1 μg/ml, for 32 hours). Red, mKO. Bar, 100 μm. (**c**) Dox-regulated Fluc expression in transfected cells. Cells from **b** were subjected to luciferase assay. Fluc levels were analyzed and fold changes by Dox of transfected cells are indicated. Error bars, SEM ($n = 3$). (**d**) Autoregulatory polycistronic expression of 2A-linked genes. Cells from **b** were analyzed by western blot using a 2A antibody. Untransfected cells were used as negative control (ctrl). Full-length blots are presented in **Supplementary Figures S1,2**. CAG, chicken β-actin promoter; Dox, doxycycline; pA, polyA signal; rAAV, recombinant adeno-associated viral vector; RANGE, **r**eversible r**A**AV-mediated **N**-cistronic **g**ene **e**xpression system; RLU, relative light unit; Syn, synapsin-1 promoter; TRE, tetracycline-responsive element; WPRE, woodchuck post-transcriptional regulatory element.

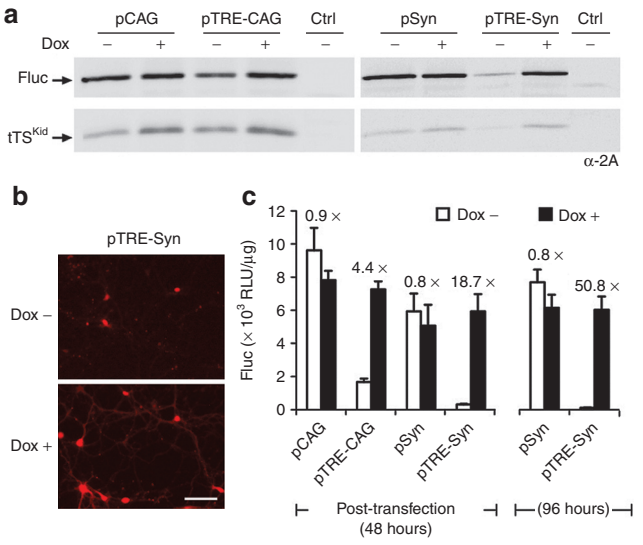

Figure 2 RANGE in transfected primary rat hippocampal neurons. (**a**) Autoregulatory polycistronic expression of 2A-linked genes. Neurons were transfected with tTS^{Kid}-based constructs and analyzed 48 hours after transfection by western blot using a 2A antibody. Untransfected neurons were used as negative control (ctrl). Full-length blots are presented in **Supplementary Figures S3,4**. (**b**) Fluorescence images of neurons transfected with pTRE-Syn construct 48 hours after transfection in the absence or presence of Dox (1 μg/ml, for 42 hours). Red, mKO. Bar, 100 μm. (**c**) Dox-regulated Fluc expression in transfected neurons. Dox (40 ng/ml) was added into culture medium 5 hours after transfection. At 48 or 96 hours after transfection, neurons were subjected to luciferase assay. Fluc levels were analyzed and fold changes by Dox of transfected neurons are indicated. Error bars, SEM (n = 3). CAG, chicken β-actin promoter; Dox, doxycycline; rAAV, recombinant adeno-associated viral vector; RANGE, **r**eversible r**A**AV-mediated **N**-cistronic **g**ene **e**xpression system; RLU, relative light unit; Syn, synapsin-1 promoter.

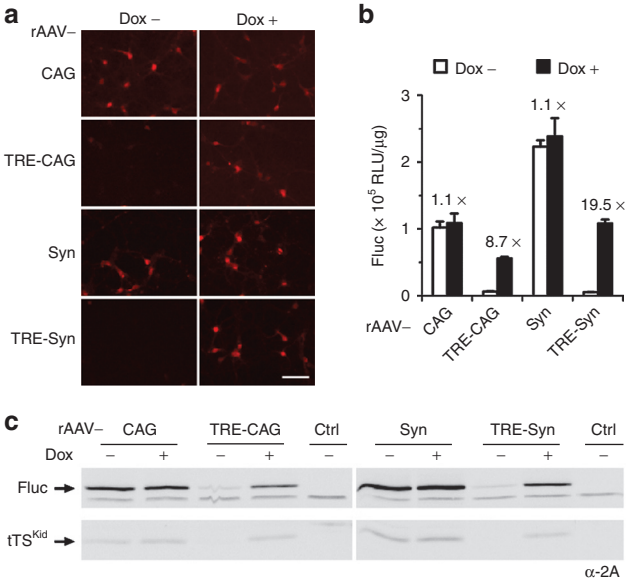

Figure 3 RANGE in infected primary rat hippocampal neurons. (**a**) Fluorescence images of primary neurons infected with tTS^{Kid}-based rAAV vectors 12 days post-infection (dpi) in the absence or presence of Dox (1 μg/ml, for 7 days). Red, mKO. Bar, 100 μm. (**b**) Dox-regulated Fluc expression in transduced neurons. Neurons from **a** were subjected to luciferase assay. Fluc levels were analyzed and fold changes by Dox of transduced neurons are indicated. Error bars, SEM (triplet). (**c**) Autoregulatory polycistronic expression of 2A-linked genes. Neurons from **a** were analyzed by western blot using a 2A antibody. Uninfected neurons were used as negative control (ctrl). Full-length blots are presented in **Supplementary Figures S5,6**. CAG, chicken β-actin promoter; Dox, doxycycline; rAAV, recombinant adeno-associated viral vector; RANGE, **r**eversible r**A**AV-mediated **N**-cistronic **g**ene **e**xpression system; RLU, relative light unit; Syn, synapsin-1 promoter; TRE, tetracycline-responsive element.

In nondividing primary (E18) rat hippocampal neurons, transfection was less efficient than in dividing HEK 293 cells, leading to lower levels of transgene expression.[30,31] After 48 hours of transfection, polycistronic regulation by Dox was observed by western blot and microscopic analysis (**Figure 2a,b**). When compared with the constitutive expression of the control constructs, the repressed Fluc levels of the conditional TRE constructs were fully regained by Dox treatment. This indicates complete Dox inactivation of tTS^{kid} in the "ON" state. The ranges of regulation between the tTS^{Kid}-mediated autorepressed state and the regained intrinsic activity of the TRE-controlled promoters were 4.4-fold (± 0.4) for the CAG and 18.7-fold (± 2.4) for the Syn promoter. On examining the Syn constructs 96 hours after transfection, we found that both the Dox-induced Fluc (pTRE-Syn, Dox +) and the constitutively expressing Fluc (pSyn, Dox – or Dox +) remained at the same level after 48 hours. However, without Dox, the basal Fluc level (pTRE-Syn, Dox –) dropped markedly between 48 and 96 hours, resulting in a much higher Fluc induction (50.8 ± 1.5-fold) by Dox compared with that after 48 hours (**Figure 2c**). This may indicate that the basal expression of the autoregulatory loop of RANGE is dynamic in the "OFF" state.

RANGE *in vitro*

For efficient gene delivery, we packaged the RANGE system as rAAV vectors. Twelve days after rAAV infection of primary neurons, Dox regulation could be observed by mKO expression (**Figure 3a**). Luc measurement revealed a Fluc value tenfold higher than that of transfected neurons, mainly due to higher infection efficiency. Nevertheless, Dox induced a Fluc increase of 8.7-fold through the TRE-controlled CAG (TRE-CAG) and of 19.5-fold through the TRE-controlled Syn (TRE-Syn) promoter (**Figure 3b**). Western blot analysis confirmed polycistronic regulation of Fluc and tTS^{Kid} by Dox (**Figure 3c**). The levels of gene expression were strictly Dox-dependent and reached a maximum at 1 μg/ml Dox concentration (**Figure 4a**). Even after a prolonged "OFF" period (10 days post-injection (dpi)), Dox induced a 5.4-fold Fluc increase through the TRE-CAG and 19.4-fold through the TRE-Syn promoter. Ten days after Dox removal, both the promoters could be repressed through tTS^{Kid} again, as Fluc had returned to baseline levels (CAG: 1.5-fold, P = 0.14; Syn: 2.4-fold, P = 0.03) (**Figure 4b,c**). These findings show that rAAV-mediated transfer of the RANGE system to neurons permits adjustable and reversible control of polycistronic gene expression.

RANGE in brain by focal gene delivery

For *in vivo* studies, Balb/C mice were subjected to bilateral rAAV injections into cortical and hippocampal regions. The conditional TRE vector (rAAV-TRE-Syn-Fluc2A-tTS^{Kid}2A-mKO) was injected into the right hemisphere and the

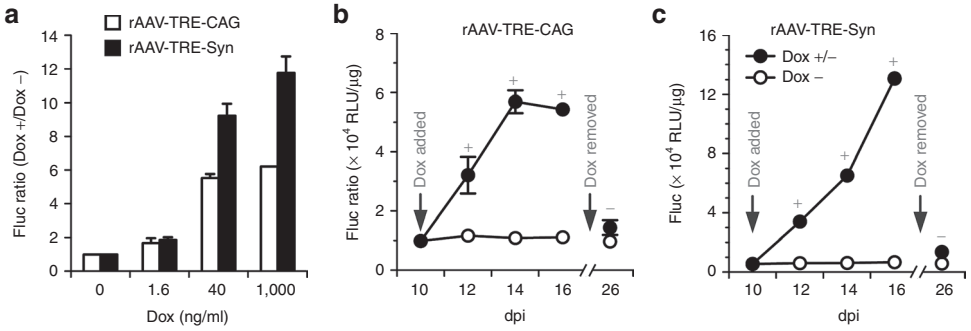

Figure 4 Adjustable and reversible control of RANGE in infected primary rat hippocampal neurons. (**a**) Dox responsiveness of transduced neurons. At 5 days post-infection (dpi), neurons were kept in the presence of indicated Dox concentrations for 5 days, and then subjected to luciferase assay. Fluc levels were analyzed and fold changes by Dox of transduced neurons were presented. Error bars, SEM ($n = 3$). (**b**,**c**) Kinetics of reversible Fluc expression in neurons infected with (**b**) rAAV-TRE-CAG or (**c**) rAAV-TRE-Syn. At 10 dpi, neurons were kept in the absence or presence of Dox (1 μg/ml); 6 days later, Dox was removed for 10 days. Neurons were subjected to luciferase assay. –, in the absence of Dox; +, in the presence of Dox. Error bars, SEM ($n = 3$). CAG, chicken β-actin promoter; Dox, doxycycline; rAAV, recombinant adeno-associated viral vector; RANGE, **r**eversible r**A**AV-mediated **N**-cistronic **g**ene **e**xpression system; RLU, relative light unit; Syn, synapsin-1 promoter; TRE, tetracycline-responsive element.

constitutive vector (rAAV-Syn-Fluc2A-tTS^{Kid}2A-mKO) into the left hemisphere. Unlike in cell culture studies, the viral transductions and protein extractions might be highly variable among individual rAAV-injected animals. Therefore, we premixed and coinjected a reference vector (rAAV-Syn-Rluc2A-Venus) with either the constitutive or the conditional rAAV vector to normalize variability using the *Renilla* luc (Rluc) expression of the reference vector (**Figure 5a**). This approach has the disadvantage that, due to trans-silencing (promoter interference and Dox upregulation of Rluc, **Supplementary Figure S7**), the Fluc induction levels were underestimated.

In rAAV-injected living mice, BLI was performed to monitor Fluc expression 14, 21, 28, 35, and 42 dpi. For the Dox-naive group (Dox –), in all five observation sessions, Fluc was restricted to the left brain hemispheres, where the constitutive vector was injected. For the Dox-treated group (Dox +/–), Fluc signals from the right brain hemispheres emerged only after Dox treatment, indicating Dox-induced Fluc expression by the conditional vector (rAAV-TRE-Syn-Fluc2A-tTS^{Kid}2A-mKO). Notably, the Fluc signals from the right hemisphere disappeared again after Dox withdrawal. The reversible regulation cycle was carried out twice in the same animals (**Figure 5a**).

For quantitative analyses at each time point, dual luc assays of Fluc and Rluc were performed using brain extracts separately prepared from the left and right hemispheres from one animal of each group. Fluc values were first normalized to Rluc values to eliminate variability in viral transduction and protein extraction. Then the ratios of normalized Luc (nLuc) levels between the right (R, conditional) and the left (L, constitutive) hemisphere were calculated, reflecting the extent of Dox regulation for each individual mouse. The nLuc (R/L) obtained from the first session was set to 1 and served as a reference point. Comparing to the Dox-naive animals, the first Dox exposure induced a 5.3-fold and the second exposure induced a 4.1-fold increase through activation of the TRE-Syn promoter in the Dox-treated animals. Seven days after Dox withdrawal, expression levels returned to the levels of the Dox-naive animals, consistent with the reversible regulation cycles observed in BLI (**Figure 5b**).

Using Venus fluorescence as a reporter for rAAV transductions in brain slices, we observed the trans-silencing of the Syn promoter by TRE-Syn-driven tTS^{Kid} from the coinjected conditional rAAV. In the right hemisphere, Syn-driven Venus expression was dependent on the Dox treatment in Dox + and Dox +/– animals, in contrast to that in the left hemisphere where only constitutive rAAVs were coinjected. Most importantly, using mKO as a reporter for Dox regulation, we could visualize Dox-dependent repression and/or activation of TRE-Syn-driven mKO expression in the right hemisphere of the untreated (Dox –), the Dox-treated (Dox +), and the Dox-withdrawn animals after two complete cycles of Dox treatment (Dox +/–) at the cellular level (**Figure 5c**,**d**).

RANGE in peripheral tissues by systemic gene delivery

To further illustrate potential applications other than brain, we delivered the RANGE vectors into Balb/C mice through tail vein injection systemically. Again, a conditional vector (rAAV-TRE-CAG-Fluc2A-tTS^{Kid}2A-mKO) was premixed with a control vector (rAAV-CMV-Rluc2A-Venus), and coinjected into the tail veins. Once rAAV transduction reached a plateau at 60 dpi,[32] BLI showed Fluc signals in liver of all infected mice. Upon Dox treatment, Fluc signals were intensified and then reduced following Dox withdrawal (**Figure 6a**). Tissue extracts of liver and hindlimb muscle were found to be transduced by rAAV using dual luc assays. Compared with the Dox-naive group (Dox –), Dox induced a 4.8-fold Fluc increase in liver and a 1.9-fold increase in muscle when normalized to Rluc, the internal reference for viral transduction (**Figure 6b**). We observed mKO-positive cells in liver slices of injected but not of uninjected mice (data not shown). Compared with the untreated (Dox –) or the Dox-withdrawn (Dox +/–) mice, there were substantially higher numbers of mKO-expressing cells in the Dox-treated mice (Dox +) (**Figure 6c**). Furthermore, mKO was found to colocalize only with 4′,6-diamidino-2-phenylindole (DAPI)-stained nuclei confirming their identity as rAAV-transduced cells (**Figure 6d**).

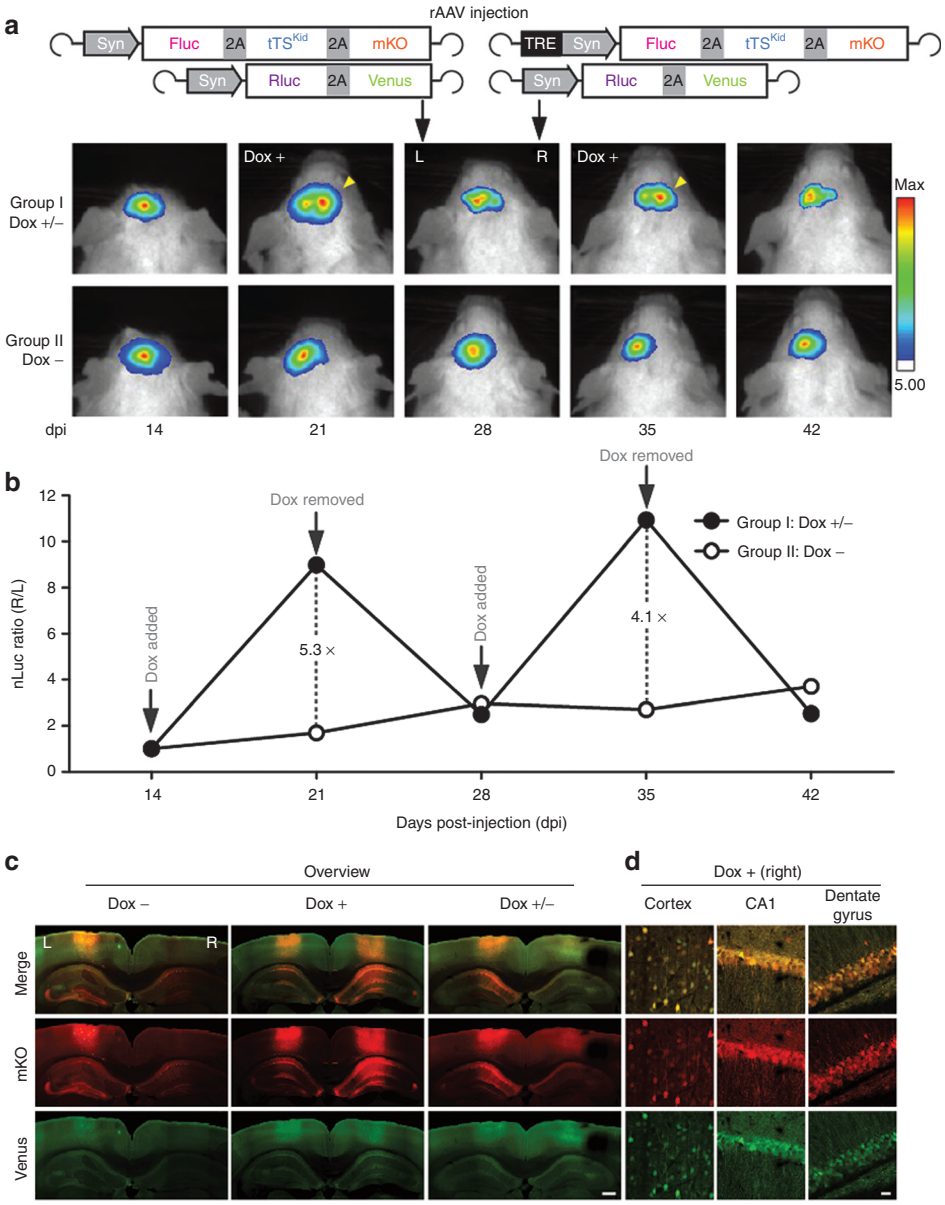

Figure 5 RANGE in mouse brain. (**a**) Bioluminescence images of Fluc in the brains of two mice bilaterally injected with indicated rAAV vectors 14, 21, 28, 35, and 42 days post-injection (dpi). One mouse (Dox +/–) went through two cycles of Dox treatment (2 mg/ml in drinking water for 7 days, then Dox withdrawal for 7 days), whereas the other was never exposed to Dox (Dox –). After Dox treatment (Dox +/–), signals from right hemisphere appeared (indicated by yellow arrowheads). The signal range was normalized and is shown from 5 to maximal photon counts per pixel. (**b**) Quantification of reversible luciferase expression in brain. Effect of Dox regulation was indicated by comparing normalized luciferase (nLuc) levels in right hemisphere to that in left hemisphere. nLuc = right (Fluc/Rluc)/left (Fluc/Rluc). Fold changes between two groups are indicated. (**c**) Fluorescence images of injected brain areas from untreated (Dox –), Dox-treated (Dox +), and Dox-withdrawn (Dox +/–) mice. Individual color channels were adjusted for better detail presentation. Red, mKO; green, Venus. Bar, 0.5 mm. (**d**) Magnified fluorescence images of selected brain regions from the right hemisphere of a Dox-treated (Dox +) mouse. Individual color channels were adjusted. Red, mKO; green, Venus. Bar, 20 µm. Dox, doxycycline; L, left; rAAV, recombinant adeno-associated viral vector; R, right; RANGE, **r**eversible r**A**AV-mediated **N**-cistronic **g**ene **e**xpression system; Syn, synapsin-1 promoter; TRE, tetracycline-responsive element.

To demonstrate the spatial control of RANGE, we used the same experimental approach, analyzing the mice that received tail vein injection of rAAV-TRE-Syn-Fluc2A-tTS^{Kid}2A-mKO. As expected, no detectable signals could be visualized by BLI in injected mice regardless of Dox, demonstrating that spatial specificity of the RANGE system is governed by the promoter as well as by the gene transfer method (**Supplementary Figure S8**).

Discussion

In this study, we designed and analyzed in detail a new, extrachromosomal, single rAAV system for spatial and reversible control of polycistronic gene expression termed RANGE. First, we systematically validated the system *in vitro* by DNA transfections as well as by rAAV infection. We showed that expression of polycistron-encoded Fluc, tTS^{Kid}, and mKO

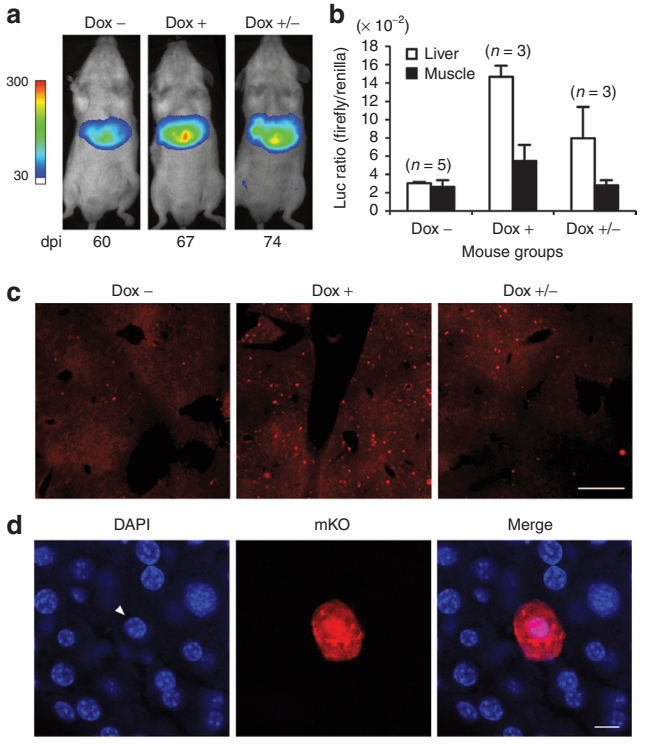

Figure 6 RANGE in peripheral tissues. (**a**) Bioluminescence images of Fluc in a mouse injected with rAAV-TRE-CAG-Fluc2A-tTS^{Kid}2A-mKO and rAAV-CMV-Rluc2A-Venus vector through tail vein before (Dox –, 60 dpi), after (Dox +, 67 dpi) Dox treatment, and after Dox withdrawal (Dox +/–, 74 dpi). The signal ranged from 30–300 photon counts per pixel. (**b**) Quantification of reversible luciferase expression in liver and muscle cells in untreated (Dox –), Dox-treated (Dox +), and Dox-withdrawn (Dox +/–) mice. Error bars, SEM. (**c**) Fluorescence images of liver sections. The number of mKO-expressing cells was higher in the Dox-treated mouse (Dox +) compared with the untreated (Dox –) or the withdrawn ones (Dox +/–). Red, mKO. Bar, 0.5 mm. (**d**) Fluorescence images of DAPI-stained liver sections. Signals of mKO were found to colocalize only with DAPI-stained nuclei, indicated by a white arrowhead. The images were pseudocolored from grayscale images with blue for DAPI and red for mKO. Individual color channels were adjusted. Blue, DAPI; red, mKO. Bar, 10 μm. CAG, chicken β-actin promoter; CMV, cytomegalovirus; dpi, days post-injection; DAPI, 4′,6-diamidino-2-phenylindole; Dox, doxycycline; rAAV, recombinant adeno-associated viral vector; R, right; RANGE, **r**eversible r**A**AV-mediated **N**-cistronic **g**ene **e**xpression system; TRE, tetracycline-responsive element.

could be repressed by tTS^{Kid}, and could be efficiently induced by Dox up to 50-fold. After focal and systemic rAAV administration of the RANGE system in the mouse, we visualized efficient tissue-specific reversible gene regulation in brain and liver of living mice by BLI.

The outstanding feature of the RANGE system is its autoregulatory machinery in which tTS^{Kid} expression is driven by TRE-controlled eukaryotic promoters. In our study, we analyzed the CAG and Syn promoter by transient transfections into HEK 293 cells or primary neurons. Note that we could not apply cotransfection of reference plasmids for normalization because we, like others, observed interference between cotransfected promoters in studies using Rluc for normalizing transfection efficiency.[33] Instead, we relied on single transfections of equal DNA quantity and summarized results from three independent experiments. By comparing expression of the conditional and the respective constitutive vector, we found that both promoters could regain their intrinsic activities (100%) upon Dox treatment, indicating complete tTS^{Kid} inactivation in the "ON" state. The quantitative comparison between the CAG and Syn promoters in the two cell types demonstrated that (i) the extent of regulation with the Syn promoter was higher than with the CAG promoter in both cell types; (ii) the extent of regulation in neurons were higher than in HEK cells for both promoters; and (iii) the extent of regulation with the Syn promoter in neurons 96 hours after transfection was higher than that after 48 hours. The first observation suggests a lower susceptibility of the ubiquitous CAG promoter to tTS^{Kid}-mediated repression compared with that of the neuron-specific Syn promoter. The second observation implies a more efficient tTS^{Kid}-mediated repression in neurons compared with dividing HEK 293 cells. The third observation reveals that the autoregulatory loop of the repressed RANGE system in the "OFF" state is dynamic over time even for a given promoter in a given cell type. Finally, we achieved a maximal 50.8-fold activation of Syn promoter in neurons, showing that the autoregulatory loop of the RANGE system can effectively reach a balanced repression state with a baseline of <2% of the intrinsic promoter activity. Taken together, our data demonstrate that the autoregulatory RANGE system is dependent on promoter selection, on cell type, and also on experimental window. Therefore, it is possible to fine-tune the RANGE system for diverse applications.

The most novel feature of the RANGE system is its polycistronic configuration achieved by the employment of 2A peptide bridges. Compared with multiple,[13–15] bidirectional promoters[9,10] or bulky internal ribosome entry site sequences,[34,35] the 2A peptide bridge contains only 54 base pairs.[24] Thanks to its small size, we could for the first time accommodate all essential regulatory components together with two reporter genes within the ~5 kb rAAV package limit. During translation, 2A self-cleaves and adds its first 17 amino acids to the N-terminal proteins Fluc and tTS^{Kid25}. We did not observe any obvious functional disruption by the C-terminal "2A-tag", either to the enzymatic activity of Fluc or to the transcriptional silencer tTS^{Kid}. Moreover, the "2A-tag" served as a useful tag for simultaneous detection of all products of 2A-linked genes in western blot analysis using a 2A antibody. More than 95% of gene products were fully cleaved (**Supplementary Figures S1–6**), indicating high efficiency of 2A-mediated cotranslational "self-cleavage". However, although the detected Fluc and the tTS^{Kid} levels were not equimolar, due to possibly different turnover rate and differential extraction of the cytoplasmic protein Fluc compared with the nuclear-targeted tTS^{Kid}, they were still comparable, implying that 2A-mediated coexpression is faithful.[24] Last but not least, our data show that the polycistronic expression of 2A-linked genes can be effectively regulated in a synchronized manner.

The *in vivo* applications of the RANGE system were mediated by rAAVs for efficient gene delivery and long-lasting gene expression. In living mice, we visualized Dox-regulated Fluc expression during "Doxy-Cycling" in

transduced tissues by BLI. For technical reasons, BLI is semiquantitative and does not allow simultaneous detection of Fluc and Rluc. For precise quantification, we killed mice after BLI and analyzed the transduced tissue *in vitro* by dual luc assays. We could show that in brain extracts the regulatory range remained stable (approximately fivefold) throughout two repeated "ON/OFF" cycles. The approximately fivefold *in vivo* induction was lower than the ~20-fold regulation in primary neurons. There are two possible explanations: (i) 7-day Dox treatment might not be sufficient for maximal activation *in vivo*; (ii) the approximately fivefold regulation might be underestimated due to a trans-silencing effect of the conditional vector on the constitutive Rluc reference vector. Indeed, we observed in infected primary neurons an approximately threefold Dox upregulation of Rluc when the reference vector was coinfected with the conditional vector (**Supplementary Figure S7**). Note that the trans-silencing effect could occur only when the constitutive and conditional vectors infected the same cells, where the two different rAAV genomes persisted episomally in heteroconcatemers.[36–38] In this configuration, the genome of the constitutive reference Rluc rAAV can be in close proximity to the TRE sequence of the conditional Fluc rAAV, and thus the Rluc expression unit can be trans-silenced by tTS^{Kid}. Microscopic analyses showed that the majority of virus-transduced cells indeed were positive for both mKO and Venus. In the mice injected in the tail vein, the CAG promoter exhibited an approximately twofold induction in muscle cells and approximately fivefold induction in liver cells with notable background activities. Despite the possible underestimation due to trans-silencing, the tail vein injection approach was not optimal for efficient targeting or transduction. Indeed, transduced cells were sparse even in the Dox-treated mice. We learned from our data that spatial control of the RANGE system is governed at two levels: (i) gene delivery methods determine the distribution of rAAV vectors over the target region where (ii) gene expression is controlled by cell type-specific promoters. For future applications and for precise targeting of the RANGE system, serotype-dependent tissue tropisms can be combined with the promoter specificity and the focal gene delivery method.[32]

Constitutive viral-mediated gene transfer suffers from high variability of viral transduction in different subjects. As a proof of principle, our data showed that the RANGE system allows both the "ON" and "OFF" state of rAAV-transduced genes to be studied in each virus-injected individual. This would overcome the obstacles of interindividual variability and would reduce the number of individuals that have to be employed for conclusive observation in a genetic study.

In summary, the RANGE system (i) integrates the advantages of the Tet-controlled transcriptional silencer tTS^{Kid} and the self-cleaving 2A peptide bridge, (ii) combines all essential regulatory components as an autoregulatory loop of minimal length, (iii) simplifies the gene delivery scheme, and (iv) regulates multiple genes in a synchronized manner. Cotransduction together with constitutive rAAV expression vector should be applied only after careful considerations. In the future, RANGE may serve as a versatile tool to deliver genes with adjustable and reversible expression for direct gene function correlation. In particular, the reversibility of anatomical and functional alteration that are caused by dominant-negative proteins identified e.g., in neurodegenerative diseases[39] or autistic disorders[40,41] can be analyzed by the RANGE system.

Materials and methods

Animal experimentation. All the experiments involving animals were conducted under the license at the Regierungspräsidium Karlsruhe 35-915.81/G-71/10 and 35-915.81/G-171/10, and according to the guidelines of the Max Planck Institutes. Efforts were made to minimize numbers of animals used.

Vector construction. We constructed all vectors using standard cloning procedures. In all vectors, an expression cassette of a size up to maximal 3.9 kb, is anchored in an rAAV backbone.[29] Detailed plasmid information has been submitted to GenBank with the following accession numbers:

pAAV-CAG-Fluc2A-tTS^{Kid}2A-mKO (BankIt1580768 BankIt 1580768 KC152483); pAAV-TRE-CAG-Fluc2A-tTS^{Kid}2A-mKO (BankIt1580743 BankIt1580743 KC152482); pAAV-Syn-Fluc2A-tTS^{Kid}2A-mKO (BankIt1533014 pAAV-hSYN-fLUC-2A-tTS-2A-KO JX006096); pAAV-TRE-Syn-Fluc2A-tTS^{Kid}2A-mKO (BankIt1580695 BankIt1580695 KC152481); pAAV-Syn-Rluc2A-Venus (BankIt1580783 BankIt1580783 KC152485); pAAV-CMV-Rluc2A-Venus (BankIt1580780 BankIt1580780 KC152484).

Cells, transfections, and infection. HEK 293 cells were cultured in minimum essential media (Invitrogen, Carlsbad, CA) supplemented with 10% fetal bovine serum (Pan-Biotech, Aidenbach, Germany), 2 mmol/l L-Glutamine (Invitrogen), and penicillin/streptomycin (Invitrogen), and were transfected in 12-well plates (1 µg DNA/well) by the calcium phosphate precipitation method.[42] Primary neurons were prepared from E18 rat hippocampi, cultured in neurobasal medium (Invitrogen) supplemented with 2% B-27 (Invitrogen), 2 mmol/l L-Glutamine (Invitrogen), penicillin/streptomycin (Invitrogen), and transfected in 24-well plates (500 ng DNA/well) at 7 days *in vitro* by Lipofectamine 2000 (Invitrogen). Primary neurons were infected in 48-well plates with rAAV vectors (5×10^9 genome copy (GC) per well) at 4 days *in vitro*.

Packaging of rAAV and rAAV titration. Chimeric rAAV vectors expressing AAV serotype 1 and 2 capsid protein were produced by transient transfection of HEK 293 cells.[43] Cells were collected 72 hours after transfection by centrifugation at 300*g* for 10 minutes, and the pellet was suspended in 10 ml of TNT extraction buffer (20 mmol/l Tris-HCl (pH 7.5), 150 mmol/l NaCl, 1% Triton X-100, 10 mmol/l $MgCl_2$) and incubated at room temperature for 10 minutes. Insoluble debris was pelleted at 2,100*g* for 10 minutes and supernatant was united with the original culture medium. After Benzonase (20 U/ml; Invitrogen) treatment at 37 °C for 1 hour, the united supernatant was filtered (0.2 µm filter unit; Renner, Dannstadt, Germany), and was loaded onto an AVB Sepharose High Performance affinity column (GE Healthcare, Piscataway, NJ). Viral particles were then eluted in 50 mmol/l glycine-HCl (pH 2.7).[44] The elution was neutralized by 100 mmol/l Tris-HCl (pH 8.0), washed three times with phosphate-buffered

saline (PBS) and concentrated using Amicon Ultra-4 centrifugal filters 100 K (Millipore, Billerica, MA). The concentrated rAAV solution was filter-sterilized (0.22 µm Millex Filter Units; Millipore) and stored at –80 °C. Genome titers were determined by real-time PCR using 7500 Real-Time PCR System (Applied Biosystems, Foster city, CA) using primers against the WPRE sequence (primer pair 5′-CTA TGT TGC TCC TTT TAC GCT ATG-3′ and 5′-TCA TAA AGA GAC AGC AAC CAG GAT-3′, and TaqMan probe 6-FAM-CCT TTG TAT CAT GCT ATT GCT TCC-MGB).

rAAV-mediated gene transfer in mice. For stereotactic brain injection,[45] we used 6 weeks old male Balb/C mice weighing 18–22 g (purchased from Charles River Laboratories, Sulzfeld, Germany). The mice received bilateral injection into cortex and hippocampus (anteroposterior, –2.1 mm; mediolateral, ±1.6 mm). In each mouse, 300 nl of rAAV-TRE-Syn-Fluc2A-tTS^{Kid}2A-mKO (1.5×10^{10} GC/µl) was injected at three depths from dura (–0.3, –0.9, and –1.5 mm) into the right hemisphere, whereas the same amount of control vector rAAV-Syn-Fluc2A-tTS^{Kid}2A-mKO was delivered into the left hemisphere. To each vector, a third vector rAAV-Syn-Rluc2A-Venus (7.5×10^8 GC/µl) was premixed and coinjected as internal control. For tail vein injection,[32] we used 8-week old male Balb/C mice weighing 20 - 25 g (purchased from Charles River Laboratories). The mice were injected in tail veins with 150 µl rAAV-TRE-CAG-Fluc2A-tTS^{Kid}2A-mKO (1×10^{11} GC) premixed with rAAV-CMV-Rluc2A-Venus (1×10^{10} GC) supplemented with 5% sorbitol (Sigma-Aldrich, St Louis, MO) by using 30-gauge needles (BD Biosciences, Franklin Lakes, NJ). The animals were warmed by infrared lamp and held in the Tail Veiner TV-150 position (Braintree Scientific, Braintree, MA).

Dox administration. For transfected cells, Dox (Sigma-Aldrich) was added into culture 16 hours post-transfection for HEK 293 cells (1 µg/ml Dox) and 6 hours post-transfection for primary neurons (40 ng/ml or 1 µg/ml Dox). For infected primary neurons, Dox (1 µg/ml) was added into culture at 10 dpi and renewed every second day. For rAAV-injected mice, we provided Dox in drinking water (2 mg/ml, renewed every third day; Sigma-Aldrich) with 5% sucrose or as food pellet (200 mg/kg, refreshed every third day; Bio-Serv, Frenchtown, NJ). Animals were single housed.

Protein extraction and quantification. Cells were washed with PBS and lysed with passive lysis buffer (Promega, Madison, WI) by shaking at room temperature for 15 minutes. rAAV-injected mice were killed by exposure to isoflurane (Baxtor, Deerfield, IL) and infected tissues were dissected. Brain tissues were homogenized with ice-cold 25 mmol/l HEPES buffer supplemented with proteinase inhibitor cocktail (Roche, Basel, Switzerland). Liver and muscle tissues were cryo-grinded by Mixer Mill MM 301 (RETSCH, Hann, Germany) and then suspended with ice-cold 25 mmol/l HEPES buffer supplemented with proteinase inhibitor cocktail (Roche). Tissue extracts were centrifuged at 13,000 rpm for 15 minutes at 4 °C. The supernatants were collected and protein concentrations were determined by Bradford Protein Assay (Bio-Rad, Hercules, CA).

Luc assay. Single luc assay was performed by using luc assay Reagent I (Promega) for Fluc, and *Renilla* GLOW-juice (PJK, Kleinblittersdorf, Germany) for Rluc. Briefly, cell lysate was mixed at a 1:5 ratio with luc assay reagent I or *Renilla* GLOW-juice in a BioFix lumi glass cuvette (Macherey-Nagel, Düren, Germany). After 10 seconds, luc activity was measured for 10 seconds using BioFix Lumi-10 luminometer (Macherey-Nagel) and displayed as relative light. The dual luc reporter assay system (Promega) was used to measure Fluc and Rluc sequentially from single samples. Tissue homogenate (20 µl) was mixed with 100 µl luc assay reagent II (Promega) in a BioFix lumi glass cuvette and measured for Fluc activity. Then 100 µl of Stop & Glo reagent (Promega) was added to the same BioFix lumi glass cuvette to quench Fluc and then measured for Rluc activity.

Western blot analysis. Proteins of cell lysates were separated by sodium dodecyl sulfate-polyacrylamide gel electrophoresis (4% stacking and 10% resolving gel) and electroblotted onto nitrocellulose membranes. Membranes were probed with polyclonal antibody against 2A peptide (1: 2,000; Millipore).[46] To visualize blots by FLA-9000 (FujiFilm, Tokyo, Japan), IRDye 800 conjugated Affinity Purified anti-Rabbit IgG (1:2,500; Rockland Immunochemicals, Gilbertsville, PA) was used as secondary antibody.

BLI. Mice were anesthetized with 1.5% isoflurane (Baxtor) in air, placed in a Photon Imager optical imaging system (Biospace Lab, Paris, France) and intraperitoneally injected with 150 mg/kg VivoGlo luciferin (Promega) dissolved in PBS. The images were acquired for 5 minutes, 3–8 minutes after luciferin administration for brain bioluminescence, and 4–9 minutes for abdominal signals. Bioluminescence signals were displayed as the number of detected photon counts per pixel.

Perfusion and section. Mice were anesthetized with isoflurane (Baxtor) and perfused intracardially with warm PBS and 4% paraformaldehyde. Brains or livers were dissected out and post-fixed in ice-cold 4% paraformaldehyde for 1 hour and sliced on a vibratome (Leica Microsystems, Wetzlar, Germany) into 50–60 µm sections. Liver sections were stained with 2 µg/ml DAPI (SERVA Electrophoresis, Heidelberg, Germany). Brain and liver sections were mounted onto slides using Aqua-Poly/Mount (Polysciences, Warrington, PA).

Microscopy. For overviews, sections were visualized by Axio Imager (Carl Zeiss, Jena, Germany), M1 microscope (Plan-Neofluar 10x/0.30 objectives, Zeiss AxioCam HR camera), and AxioVision software (Zeiss, release 4.8.2) for image acquisition. For detailed images, brain sections were visualized by Leica TCS SP2 confocal microscope (HC PL APO CS 20.0 × 0.70 IMM/COR objective) and Leica confocal software; liver sections were visualized by Leica TCS SP5 confocal microscope (HCX PL APO lambda blue 20 × 0.7 IMM objective) and Leica Microsystems LAS AF-TCS SP5 software (Leica Microsystems).

Statistical analysis. Using Prism 5 (GraphPad Software, La Jolla, CA), we subjected Fluc levels of cell lysates to unpaired two-tailed *t*-test, and applied a significance level of $P < 0.05$ for all statistical analyses.

Equipments and settings. All images were acquired at room temperature with the following acquisition parameters.

Figure	Pixel dimensions	Image bit depth	Fluorochromes	Reflectors
1b	1,388 × 1,040	RGB, 24 bit	mKO (548/559 nm)	Rhodamine (540/580 nm)
2b	1,388 × 040	RGB, 24 bit	mKO (548/559 nm)	Rhodamine (540/580 nm)
3a	1,388 × 1,040	RGB, 24 bit	mKO (548/559 nm)	Rhodamine (540/580 nm)
5c	5,068 × 3,329 4,094 × 2,318 5,526 × 4,081	RGB, 24 bit	Venus (515/528 nm) mKO (548/559 nm)	FITC (495/525 nm) Rhodamine (540/580 nm)
5d	1,024 × 1,024	RGB, 24 bit	Venus (515/528 nm) mKO (548/559 nm)	YFP (517/535 nm) TRITC (555/625 nm)
6c	2,736 × 1,292 2,061 × 1,292 2,736 × 3,313	RGB, 24 bit	mKO (548/559 nm)	Rhodamine (540/580 nm)
6d	1,024 × 1,024	Grayscale, 8 bit	DAPI (358/461 nm) mKO (548/559 nm)	Alexa 405 (401/422 nm) DsRed (545/572 nm)

All images were processed using Adobe Photoshop CS5 (Adobe Systems, San Jose, CA). Due to space limits, Figures 1b,2b,3a,5c and 6c were subjected to cropping or size reduction. For better image display, all images were subjected to brightness/contrast adjustment or γ-correction. All processing was applied equally across the entire image as well as the entire subfigure.

Supplementary material

Figures S1,2. Full-length western blots of **Figure 1d**.
Figures S3,4. Full-length western blots of **Figure 2a**.
Figures S5,6. Full-length western blots of **Figure 3c**.
Figure S7. Trans-silencing effect of coinfected rAAV vectors in primary neurons.
Figure S8. Systemic delivery of the neuron-specific RANGE.

Acknowledgments. We thank Karin Leotta (German Cancer Research Center) for assistance in bioluminescence imaging (BLI); Uwe Haberkorn (University Hospital of Heidelberg and German Cancer Research Center) for providing BLI facility; Jing Ni (German Cancer Research Center) for tail vein injections; Sabine Grünewald and Areej Albariri for culturing cells; Jun Zhou (German Cancer Research Center), Günter Giese and Annemarie Scherbarth for help with Leica TCS microscope; Mazahir T. Hasan for providing plasmid pUHS6-1 and initial discussion. We thank Neil M. Fournier (Yale University) and John Wray for critical reading and language editing of the manuscript. We thank Peter H. Seeburg for his generous support and strong interest in conditional gene regulation systems. Y.C. received a MPI PhD fellowship. This work was supported by the Max Planck Society. The authors declared no conflict of interest.

1. Davidson, BL and Breakefield, XO (2003). Viral vectors for gene delivery to the nervous system. *Nat Rev Neurosci* **4**: 353–364.
2. Mingozzi, F and High, KA (2011). Therapeutic in vivo gene transfer for genetic disease using AAV: progress and challenges. *Nat Rev Genet* **12**: 341–355.
3. Summerford, C and Samulski, RJ (1999). Viral receptors and vector purification: new approaches for generating clinical-grade reagents. *Nat Med* **5**: 587–588.
4. Grimm, D, Kay, MA and Kleinschmidt, JA (2003). Helper virus-free, optically controllable, and two-plasmid-based production of adeno-associated virus vectors of serotypes 1 to 6. *Mol Ther* **7**: 839–850.
5. Gossen, M and Bujard, H (1992). Tight control of gene expression in mammalian cells by tetracycline-responsive promoters. *Proc Natl Acad Sci USA* **89**: 5547–5551.
6. Gossen, M, Freundlieb, S, Bender, G, Müller, G, Hillen, W and Bujard, H (1995). Transcriptional activation by tetracyclines in mammalian cells. *Science* **268**: 1766–1769.
7. Lewandoski, M (2001). Conditional control of gene expression in the mouse. *Nat Rev Genet* **2**: 743–755.
8. Sprengel, R and Hasan, MT (2007). Tetracycline-controlled genetic switches. *Handb Exp Pharmacol*: 49–72.
9. Vanrell, L, Di Scala, M, Blanco, L, Otano, I, Gil-Farina, I, Baldim, V *et al.* (2011). Development of a liver-specific Tet-on inducible system for AAV vectors and its application in the treatment of liver cancer. *Mol Ther* **19**: 1245–1253.
10. Fitzsimons, HL, Mckenzie, JM and During, MJ (2001). Insulators coupled to a minimal bidirectional tet cassette for tight regulation of rAAV-mediated gene transfer in the mammalian brain. *Gene Ther* **8**: 1675–1681.
11. Haberman, R, Criswell, H, Snowdy, S, Ming, Z, Breese, G, Samulski, R *et al.* (2002). Therapeutic liabilities of in vivo viral vector tropism: adeno-associated virus vectors, NMDAR1 antisense, and focal seizure sensitivity. *Mol Ther* **6**: 495–500.
12. McGee Sanftner, LH, Rendahl, KG, Quiroz, D, Coyne, M, Ladner, M, Manning, WC *et al.* (2001). Recombinant AAV-mediated delivery of a tet-inducible reporter gene to the rat retina. *Mol Ther* **3**(5 Pt 1): 688–696.
13. Stieger, K, Le Meur, G, Lasne, F, Weber, M, Deschamps, JY, Nivard, D *et al.* (2006). Long-term doxycycline-regulated transgene expression in the retina of nonhuman primates following subretinal injection of recombinant AAV vectors. *Mol Ther* **13**: 967–975.
14. Lhériteau, E, Libeau, L, Mendes-Madeira, A, Deschamps, JY, Weber, M, Le Meur, G *et al.* (2010). Regulation of retinal function but nonrescue of vision in RPE65-deficient dogs treated with doxycycline-regulatable AAV vectors. *Mol Ther* **18**: 1085–1093.
15. Campbell, M, Humphries, MM, Kiang, AS, Nguyen, AT, Gobbo, OL, Tam, LC *et al.* (2011). Systemic low-molecular weight drug delivery to pre-selected neuronal regions. *EMBO Mol Med* **3**: 235–245.
16. Gafni, Y, Pelled, G, Zilberman, Y, Turgeman, G, Apparailly, F, Yotvat, H *et al.* (2004). Gene therapy platform for bone regeneration using an exogenously regulated, AAV-2-based gene expression system. *Mol Ther* **9**: 587–595.
17. Wang, JJ, Niu, DB, Zhang, T, Wang, K, Xue, B and Wang, XM (2005). A tetracycline-regulatable adeno-associated virus vector for double-gene transfer. *Neurosci Lett* **378**: 106–110.
18. Cambridge, SB, Geissler, D, Calegari, F, Anastassiadis, K, Hasan, MT, Stewart, AF *et al.* (2009). Doxycycline-dependent photoactivated gene expression in eukaryotic systems. *Nat Methods* **6**: 527–531.
19. Rendahl, KG, Quiroz, D, Ladner, M, Coyne, M, Seltzer, J, Manning, WC *et al.* (2002). Tightly regulated long-term erythropoietin expression in vivo using tet-inducible recombinant adeno-associated viral vectors. *Hum Gene Ther* **13**: 335–342.
20. Haberman, RP and McCown, TJ (2002). Regulation of gene expression in adeno-associated virus vectors in the brain. *Methods* **28**: 219–226.
21. Freundlieb, S, Schirra-Müller, C and Bujard, H (1999). A tetracycline controlled activation/repression system with increased potential for gene transfer into mammalian cells. *J Gene Med* **1**: 4–12.
22. Margolin, JF, Friedman, JR, Meyer, WK, Vissing, H, Thiesen, HJ and Rauscher, FJ 3rd (1994). Kruppel-associated boxes are potent transcriptional repression domains. *Proc Natl Acad Sci USA* **91**: 4509–4513.
23. Witzgall, R, O'Leary, E, Leaf, A, Onaldi, D and Bonventre, JV (1994). The Kruppel-associated box-A (KRAB-A) domain of zinc finger proteins mediates transcriptional repression. *Proc Natl Acad Sci USA* **91**: 4514–4518.
24. Tang, W, Ehrlich, I, Wolff, SB, Michalski, AM, Wölfl, S, Hasan, MT *et al.* (2009). Faithful expression of multiple proteins via 2A-peptide self-processing: a versatile and reliable method for manipulating brain circuits. *J Neurosci* **29**: 8621–8629.
25. Donnelly, ML, Luke, G, Mehrotra, A, Li, X, Hughes, LE, Gani, D *et al.* (2001). Analysis of the aphthovirus 2A/2B polyprotein 'cleavage' mechanism indicates not a proteolytic reaction, but a novel translational effect: a putative ribosomal 'skip'. *J Gen Virol* **82**(Pt 5): 1013–1025.
26. Karasawa, S, Araki, T, Nagai, T, Mizuno, H and Miyawaki, A (2004). Cyan-emitting and orange-emitting fluorescent proteins as a donor/acceptor pair for fluorescence resonance energy transfer. *Biochem J* **381**(Pt 1): 307–312.
27. Sawicki, JA, Morris, RJ, Monks, B, Sakai, K and Miyazaki, J (1998). A composite CMV-IE enhancer/beta-actin promoter is ubiquitously expressed in mouse cutaneous epithelium. *Exp Cell Res* **244**: 367–369.
28. Kügler, S, Kilic, E and Bähr, M (2003). Human synapsin 1 gene promoter confers highly neuron-specific long-term transgene expression from an adenoviral vector in the adult rat brain depending on the transduced area. *Gene Ther* **10**: 337–347.
29. Shevtsova, Z, Malik, JM, Michel, U, Bähr, M and Kügler, S (2005). Promoters and serotypes: targeting of adeno-associated virus vectors for gene transfer in the rat central nervous system in vitro and in vivo. *Exp Physiol* **90**: 53–59.
30. Jordan, M and Wurm, F (2004). Transfection of adherent and suspended cells by calcium phosphate. *Methods* **33**: 136–143.
31. Ohki, EC, Tilkins, ML, Ciccarone, VC and Price, PJ (2001). Improving the transfection efficiency of post-mitotic neurons. *J Neurosci Methods* **112**: 95–99.

32. Zincarelli, C, Soltys, S, Rengo, G and Rabinowitz, JE (2008). Analysis of AAV serotypes 1-9 mediated gene expression and tropism in mice after systemic injection. *Mol Ther* **16**: 1073–1080.
33. Shifera, AS and Hardin, JA (2010). Factors modulating expression of Renilla luciferase from control plasmids used in luciferase reporter gene assays. *Anal Biochem* **396**: 167–172.
34. Sudol, KL, Mastrangelo, MA, Narrow, WC, Frazer, ME, Levites, YR, Golde, TE *et al.* (2009). Generating differentially targeted amyloid-beta specific intrabodies as a passive vaccination strategy for Alzheimer's disease. *Mol Ther* **17**: 2031–2040.
35. Szulc, J, Wiznerowicz, M, Sauvain, MO, Trono, D and Aebischer, P (2006). A versatile tool for conditional gene expression and knockdown. *Nat Methods* **3**: 109–116.
36. Fisher, KJ, Jooss, K, Alston, J, Yang, Y, Haecker, SE, High, K *et al.* (1997). Recombinant adeno-associated virus for muscle directed gene therapy. *Nat Med* **3**: 306–312.
37. Nakai, H, Storm, TA and Kay, MA (2000). Recruitment of single-stranded recombinant adeno-associated virus vector genomes and intermolecular recombination are responsible for stable transduction of liver in vivo. *J Virol* **74**: 9451–9463.
38. McCarty, DM, Young, SM Jr and Samulski, RJ (2004). Integration of adeno-associated virus (AAV) and recombinant AAV vectors. *Annu Rev Genet* **38**: 819–845.
39. Teplow, D (2012). Molecular Biology of Neurodegenerative Diseases. Academic Press: Salt lake city. pp. 498.
40. Berkel, S, Marshall, CR, Weiss, B, Howe, J, Roeth, R, Moog, U *et al.* (2010). Mutations in the SHANK2 synaptic scaffolding gene in autism spectrum disorder and mental retardation. *Nat Genet* **42**: 489–491.
41. Berkel, S, Tang, W, Treviño, M, Vogt, M, Obenhaus, HA, Gass, P *et al.* (2012). Inherited and de novo SHANK2 variants associated with autism spectrum disorder impair neuronal morphogenesis and physiology. *Hum Mol Genet* **21**: 344–357.
42. Chen, C and Okayama, H (1987). High-efficiency transformation of mammalian cells by plasmid DNA. *Mol Cell Biol* **7**: 2745–2752.
43. Klugmann, M, Symes, CW, Leichtlein, CB, Klaussner, BK, Dunning, J, Fong, D *et al.* (2005). AAV-mediated hippocampal expression of short and long Homer 1 proteins differentially affect cognition and seizure activity in adult rats. *Mol Cell Neurosci* **28**: 347–360.
44. Smith, RH, Levy, JR and Kotin, RM (2009). A simplified baculovirus-AAV expression vector system coupled with one-step affinity purification yields high-titer rAAV stocks from insect cells. *Mol Ther* **17**: 1888–1896.
45. Cetin, A, Komai, S, Eliava, M, Seeburg, PH and Osten, P (2006). Stereotaxic gene delivery in the rodent brain. *Nat Protoc* **1**: 3166–3173.
46. Fang, J, Qian, JJ, Yi, S, Harding, TC, Tu, GH, VanRoey, M *et al.* (2005). Stable antibody expression at therapeutic levels using the 2A peptide. *Nat Biotechnol* **23**: 584–590

Supplementary Information accompanies this paper on the Molecular Therapy–Nucleic Acids website (http://www.nature.com/mtna)